TISSUE ENGINEERING: Part A
Volume 28, Numbers 19 and 20, 2022

DOI: 10.1089/ten.tea.2022.0049

termis
Tissue Engineering
& Regenerative Medicine
International Society

ORIGINAL ARTICLE

Induction of Cartilage Regeneration by Nanoparticles Loaded with Dentin Matrix Extracted Proteins

Sicong Mao,[1] Sainan Wang, PhD,[1] Yuting Niu, PhD,[2] Jilin Wu, PhD,[1] Peipei Jia,[1]
Jinxuan Zheng, PhD,[3] and Yanmei Dong, DDS, PhD[1]

Due to the limited self-repair capacity of articular cartilage, tissue engineering has good application prospects for cartilage regeneration. Dentin contains several key growth factors involved in cartilage regeneration. However, it remains unknown whether dentin matrix extracted proteins (DMEP) can be utilized as a complex growth factor mixture to induce cartilage regeneration. In this work, we extracted DMEP from human dentin and improved the content and activity of chondrogenic-related growth factors in DMEP by alkaline conditioning. Afterward, mesoporous silica nanoparticles (MSNs) with particular physical and chemical properties were composed to selectively load and sustain the release of proteins in DMEP. MSN-DMEP promoted chondrogenic differentiation of rat bone marrow-derived mesenchymal stem cells with fewer growth factors than exogenously added transforming growth factor-β1 (TGF-β1). Therefore, MSN-DMEP may serve as a promising candidate for cartilage regeneration as an alternative to expensive synthetic growth factors.

Keywords: dentin matrix extracted protein, mesoporous silica nanoparticles, transforming growth factor-β1, chondrogenic differentiation, cartilage regeneration

Impact Statement

Several growth factors embedded in dentin matrix could be involved in cartilage regeneration. This article reports that alkaline conditioning could improve the content and activity of chondrogenic-related growth factors in dentin matrix extracted proteins (DMEP). Mesoporous silica nanoparticles (MSNs) with particular physical and chemical properties performed well in loading and sustained releasing of proteins in DMEP. *In vitro* and *in vivo* studies suggest that MSN-DMEP could be a promising candidate for cartilage regeneration as an alternative to expensive synthetic growth factors.

Introduction

Articular cartilage is a highly specialized tissue that lacks blood vessels and nerves and has limited self-repair ability. The repair and regeneration of articular cartilage have always been a challenge in clinical practice.[1] In recent years, with deepening research in the fields of cell biology, biochemistry and bioactive materials, tissue engineering has become a promising solution for cartilage regeneration.[2] In cartilage regenerative medicine, growth factors are commonly used to induce chondrogenic differentiation of stem cells, such as transforming growth factor-β (TGF-β), insulin-like growth factor (IGF), basic fibroblast growth factor (bFGF), and bone morphogenetic protein (BMP).[3] However, a cocktail of growth factors is required to properly sequence chondrogenesis, and the delivery of one or two kinds of growth factors may be insufficient in a reparative procedure.[4] In addition, the extraction process of

Departments of [1]Cariology and Endodontology and [2]Prosthodontics, Peking University School and Hospital of Stomatology, Beijing, China.
[3]Department of Orthodontics, Hospital of Stomatology, Sun Yat-sen University, Guangdong Provincial Key Laboratory of Stomatology, Guangzhou, Guangdong, China.

recombinant growth factors has strict technical requirements, and the processing, preservation, storage, and transportation of growth factors are associated with substantial costs.

Dentin contains a large number of bioactive molecules that play an important role in tooth development. It was reported that a demineralized dentin matrix can induce mesenchymal cells derived from embryonic muscle to differentiate into chondrocytes.[5,6] This effect may be associated with the noncollagenous protein in the dentin matrix.[7] Dentin matrix extracted proteins (DMEP) is a mixture of bioactive proteins extracted from demineralized dentin matrix, including a variety of growth factors, such as TGF-β,[8–10] IGF,[9–11] bFGF,[12] and BMP.[13,14] These growth factors have been confirmed to be important in cartilage development and metabolism and have a synergistic effect on the induction of chondrogenesis.[15–17] Hence, DMEP may serve as a suitable biological source of complex growth factor mixtures for promoting cartilage regeneration.

In addition, our previous study found that alkaline treatment can activate latent TGF-β in DMEP and promote cell chemotaxis. Therefore, alkaline conditioning during DMEP extraction may be a simple and effective way to further enhance the chondrogenic inductive ability of DMEP.

Bioactive material loading and slow release of target growth factors to maintain effective concentrations and durations are important for tissue engineering. As DMEP is a mixture of proteins, the design of biomaterials should facilitate the adsorption and release of complex chondrogenic-related growth factors in DMEP. The physicochemical properties of biomaterials determine their loading and release performance.[18–20] Mesoporous silica nanoparticles (MSNs) have the characteristics of high biocompatibility, large specific surface area, and controllable pore size and have attracted extensive attention for their application in drug and protein delivery.[21–24] Silicon and silica nanoparticles dissolve in biological media, leading to a silicic acid byproduct,[25,26] which plays a positive role in regulating the process of bone and cartilage formation.[27,28] MSNs with suitable physical and chemical properties may selectively load and release these chondrogenic-related growth factors in DMEP and have potential applications in cartilage tissue engineering.

In this study, we hypothesized that a modified extraction protocol could increase the activity and concentration of chondrogenic-related growth factors in DMEP. By designing MSNs with suitable physicochemical properties, the complex growth factor mixture in DMEP could be effectively loaded and sustainedly released to synergistically promote cartilage regeneration.

Materials and Methods

DMEP extraction and analysis

Extraction of DMEP. Freshly extracted, noncarious human teeth were collected from the Department of Oral and Maxillofacial Surgery, Peking University School and Hospital of Stomatology, approved by the Biomedical Ethics Committee of Peking University School of Stomatology. Soft tissues, cementum, and enamel were removed from the tooth. The remaining dentin matrices were ground into powder with the treatment of liquid nitrogen. The dentin powder was decalcified for 10 min with a 17% EDTA (Solarbio, Beijing, China) solution (pH 7.4). The dentin powder was then extracted with phosphate-buffered saline (PBS; pH 7.4; Solarbio) at 1 g/mL and 4°C for 24 h. The extracts were dialyzed with distilled water for 24 h. Then, the freeze-drying process was performed to obtain neutral solution-extracted DMEP (nDMEP). Basic solution-extracted DMEP (bDMEP) was obtained with the same protocol, except that the extracted solution was replaced with sodium carbonate–sodium bicarbonate buffer (Na_2CO_3-$NaHCO_3$; pH 10; Solarbio).

Analysis of growth factors and the total protein concentration in DMEP. The total protein concentrations in nDMEP and bDMEP were quantified using a BCA kit (Solarbio). The levels of TGF-β1 and TGF-β3 were assayed with an enzyme-linked immunosorbent assay (ELISA) kit (R&D Systems, Minneapolis, MN) according to the kit instruction manual, except that the sample activation step was omitted. The concentrations of IGF, bFGF, BMP-2, BMP-9, and vascular endothelial growth factor (VEGF) were assayed with ELISA kits (R&D Systems) strictly according to the manufacturer's instructions.

Physicochemical and biological characteristics of selected MSNs

Morphology and structure of MSNs. MSNs were synthesized as described previously.[29] Detailed information can be found in Supplementary Data. The morphology of the MSNs was investigated using transmission electron microscopy (TEM, JEM-1011; JEOL) at an acceleration voltage of 100 kV. The N_2 adsorption–desorption isotherms and pore size distributions were characterized by using a specific surface and pore size distribution analyzer (Nova 4200e; Quantachrome).

Degradation tests of MSNs. MSNs were resuspended in PBS at a concentration of 1 mg/mL. After 1, 2, and 4 weeks of incubation in a humidified incubator at 37°C, the samples were centrifuged at 16,000 rpm to collect the nanoparticles. The resulting nanoparticles were imaged with TEM. Rat bone marrow mesenchymal stem cells (rBMMSCs) were cultured with 1 mg/mL of MSN in a CO_2 incubator (5% CO_2, 37°C) for 1 week. Then, the nanoparticles were collected and imaged with TEM (the extraction and culturing methods of rBMMSCs are presented in Supplementary Data).

Cytotoxicity of MSNs. The cytotoxicity of the MSNs was determined by cell counting kit-8 (CCK-8) (Solarbio) assay. rBMMSCs were plated in the wells of a 96-well plate and allowed to attach for 24 h. Culture medium was then removed, and a medium mixed with MSNs at concentrations of 0, 0.1, 0.5, 1, and 10 mg/mL was added. After coculture for 1, 4, 7, and 14 days, 100 μL of 10% CCK-8 reagent was added to each well and incubated for an additional 2 h. Finally, the absorbance was detected with a microplate reader (EnSpire; PerkinElmer) at a wavelength of 490 nm.

Protein loading and release of MSN-DMEP

Cytochrome C (Cyto-C; Solarbio), which has a molecular weight and isoelectric point similar to those of important

growth factors in DMEP (such as TGF-β1, IGF-1 and bFGF), was selected as the model protein for the evaluation of protein loading and release. The amount of Cyto-C adsorbed onto MSN and the concentration of Cyto-C released at different time intervals was analyzed at a wavelength of 520 nm using a microplate multimodal reader. Excess DMEP was added to 1 mg of MSNs and incubated at 4°C for 24 h. After encapsulation of DMEP, the MSNs were centrifuged and washed three times. All supernatants and wash solutions were collected. The MSNs fully loaded with nDMEP (MSN-nDMEP) and MSNs fully loaded with bDMEP (MSN-bDMEP) were used for the subsequent *in vitro* and *in vivo* experiments. For the quantification of the encapsulated protein and TGF-β1, a BCA kit and an ELISA kit against human TGF-β1 were used as described above.

Cell viability of rBMMSCs cultured with MSN-DMEP

rBMMSCs were seeded at a density of 5000 cells/well in 200 μL of mesenchymal stem cell medium (MSCM) into 96-well plates. After 24 h, the medium was completely removed from each well. Then, 1 mg/mL of MSNs, 1 mg/mL of MSN-nDMEP, and 1 mg/mL of MSN-bDMEP were added and incubated at 37°C and 5% CO_2. Biocompatibility was determined by the CCK-8 assay as described previously.

Chondrogenic induction of rBMMSCs

Chondrogenic differentiation was carried out in a pellet culture system in a chondrogenic inductive medium (CIM; detailed information in Supplementary Data). We separately added 10 ng/mL of recombinant TGF-β1 (Novoprotein Biotech, Shanghai, China) and 1 mg/mL of MSN, MSN-nDMEP, or MSN-bDMEP to the medium of each experimental group and then formed chondrogenic pellets. Pellets in the TGF-β group were incubated in CIM with 10 ng/mL of TGF-β1, while pellets in the other groups were cultured in CIM. The medium was exchanged every second day over a period of 14 or 21 days.

Gene expression analysis

After 14 days of chondrogenic differentiation induction, total RNA from chondrogenic pellets was isolated with the TRIzol reagent (Thermo Fisher Scientific). The isolation was carried out according to the manufacturer's manual. Two hundred nanograms of total RNA (2000 ng) was used for a reverse transcription reaction with a complementary DNA (cDNA) reverse transcription kit (TaKaRa). The primers used to carry out the quantitative PCR (qPCR) analysis were predesigned (Sangon Biotech) (Supplementary Table S1). Quantitative real-time PCR was performed using a Qiagen miScript SYBR green PCR Kit on an ABI 7500 instrument (Applied Biosystems) following the manufacturer's instructions. The data were analyzed with the $2^{-\Delta\Delta Ct}$ method. There were three replicate samples for each group.

Histological staining

After 21 days of culture, the pellets were fixed in 4% paraformaldehyde solution (Solarbio), dehydrated with an ascending ethanol gradient, embedded in paraffin, and sectioned into 5-μm-thick slices. Hematoxylin and eosin (HE) staining was performed according to the standard HE protocol (Solarbio). The sections were stained with safranin O (Solarbio) and alcian blue (Solarbio) according to the manufacturer's instructions.

In vivo *study*

All animal experiments were approved by the Institutional Animal Care and Use Committee of Peking University Health Science Center. Articular cartilage defects were created in both knees of New Zealand white rabbits (weight: 2.0–2.5 kg; $n=3$ per group). Rabbits were anesthetized with 10% chloral hydrate. Defects of 3.0 mm depth and 5.0 mm diameter were created in the middle of the articular cartilage of the femoral trochlea. The rabbits were randomly divided into four groups as follows: blank group, nothing was implanted into the defects; collagen (C) group, 60 μL of collagen I was implanted into the defects; collagen+MSN (C+S) group, 60 μL of collagen I with 10 mg/mL of MSN was implanted into the defects; and collagen+MSN-bDMEP (C+S+D) group, 60 μL of collagen I with 10 mg/mL of MSN-bDMEP (MSNs with maximum loading of bDMEP) was implanted into the defects. After operation, joints were closed with suture.

Rabbits were sacrificed at 12 weeks after surgery. The whole knee joints were dissected and fixed in a 4% paraformaldehyde solution for 24 h. Subsequently, the tissues were decalcified with 10% (w/v) EDTA and embedded in paraffin. Sections were cut at a thickness of 5 μm. Then HE and alcian blue staining was performed as described above. Safranin O-fast green staining (Solarbio) was performed according to the manufacturer's instructions.

Statistical analysis

SPSS 26.0 software (IBM Corp., Armonk, NY) was used for data analysis. Measurement data are presented as the mean ± standard deviation. Data were analyzed by one-way analysis of variance and Student's unpaired *t*-test. A p-value <0.05 was selected as the level of statistical significance.

Results

DMEP extracted in basic buffer increased growth factor content

DMEP extracted in neutral and basic solutions was analyzed by BCA and ELISA experiments. There was no significant difference in the total protein content of DMEP extracted in bDMEP (0.232 ± 0.063 mg/mL) and in nDMEP (0.194 ± 0.063 mg/mL). Nevertheless, the concentrations of TGF-β1, bFGF, and IGF-1 in bDMEP were significantly higher than those in nDMEP. The concentrations of TGF-β1, bFGF, and IGF in bDMEP were 4.35 ± 0.56, 4.58 ± 0.92, and 9.18 ± 1.36 ng/mL, respectively. In nDMEP, the concentrations of TGF-β1, bFGF, and IGF were 1.32 ± 0.62, 1.85 ± 0.71, and 4.26 ± 1.64 ng/mL, respectively (Fig. 1). In nDMEP, the concentrations of BMP-2, VEGF, and TGF-β3 were 86.63 ± 150.05, 6.63 ± 2.81, and 3.23 ± 5.60 pg/mL, respectively, while in bDMEP, the concentrations of BMP-2 and VEGF were 50.27 ± 79.90 and 5.43 ± 1.42 pg/mL.

TGF-β3 was not detectable in bDMEP, and BMP-9 was not detectable in either nDMEP or in bDMEP. The concentrations of BMP-2, VEGF, and TGF-β3 were not significantly different between nDMEP and bDMEP.

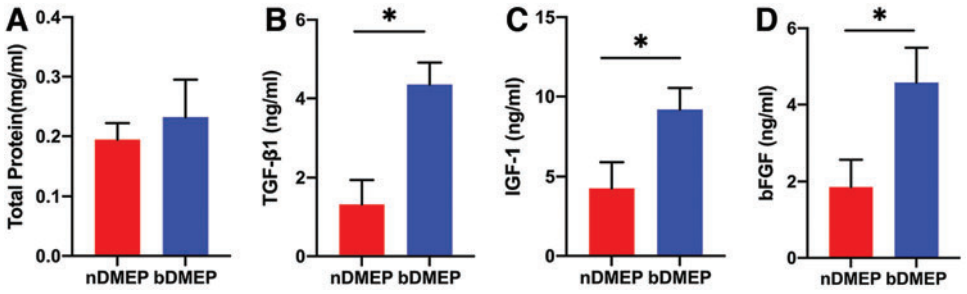

FIG. 1. Concentrations of total protein and growth factors in nDMEP and bDMEP. **(A)** Concentration of total protein. **(B)** Concentration of TGF-β1. **(C)** Concentration of bFGF. **(D)** Concentration of IGF-1. Each bar represents the mean ± SD. *$p < 0.05$. bDMEP, basic solution-extracted DMEP; bFGF, basic fibroblast growth factor; DMEP, dentin matrix extracted proteins; IGF, insulin-like growth factor; nDMEP, neutral solution-extracted DMEP; SD, standard deviation; TGF-β1, transforming growth factor-β1. Color images are available online.

Characteristics of MSNs

Morphology and structure of MSNs. TEM (Fig. 2A, B) showed that the MSNs were spherical and had a radially mesoporous structure. The particle sizes of the MSNs were 135.70 ± 12.68 nm. The N_2 adsorption–desorption isotherm of MSN (Fig. 2C) exhibits the type IV isotherm and H1 hysteresis loop, indicating a three-dimensional mesoporous channel structure with a main pore size of 6 nm (Fig. 2D).

Degradation of MSNs. We first investigated the degradability of MSNs by dispersing the particles in PBS for 4 weeks. TEM images showed that after immersion in PBS, MSNs basically maintained their original morphology, and the mesoporous structures were still clear at 1–2 weeks, indicating that MSNs were not significantly degraded (Fig. 3A–C). After 4 weeks of incubation in PBS, MSNs showed blurred boundaries, and the mesoporous structure partially disappeared (Fig. 3D). In contrast, after 1 week of coculture with rBMMSCs, MSNs showed blurred edges and collapsed mesoporous structures (Fig. 3E). These results indicated that MSNs were able to be slowly degraded in PBS and that the existence of rBMMSCs could accelerate the degradation process of MSNs.

Cell viability of rBMMSCs cultured with MSNs. The results of the CCK-8 assay showed that 0.1 mg/mL of MSNs did not affect the cell viability over 14 days of incubation in comparison with the control group (0 mg/mL). MSNs at 0.5 and 1 mg/mL decreased the cell number at 1, 4, and 7 days compared with the control group, but the inhibitory effects disappeared after 14 days of incubation. In contrast, 10 mg/mL of MSNs consistently inhibited cell viability over 14 days of incubation (Fig. 4). Therefore, 1 mg/mL of MSNs was chosen for the subsequent experiments.

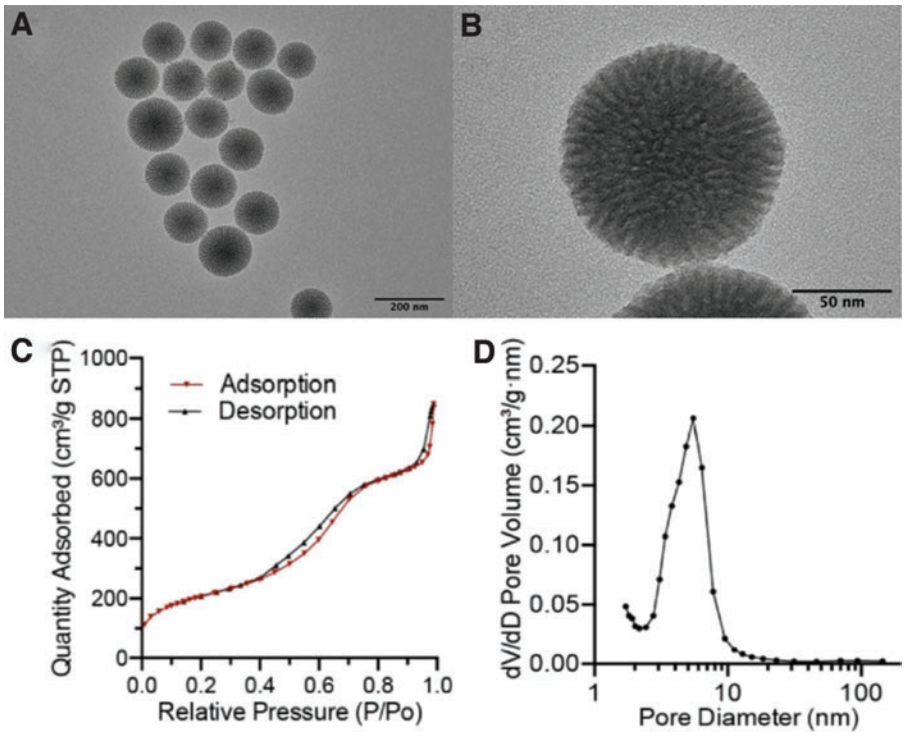

FIG. 2. Characterization of MSNs. **(A, B)** TEM images of MSNs. **(C)** Nitrogen adsorption–desorption isotherms of MSNs. **(D)** Pore size distribution curves of MSNs. MSNs, mesoporous silica nanoparticles; TEM, transmission electron microscopy. Color images are available online.

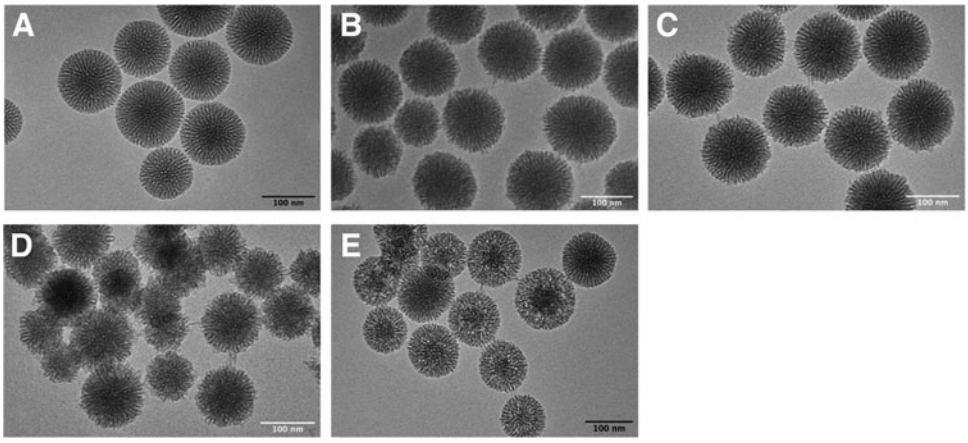

FIG. 3. Degradation of MSNs *in vitro*. **(A)** TEM image of MSNs before degradation. **(B–D)** TEM images of MSNs in PBS at 1 week **(B)**, 2 weeks **(C)**, and 4 weeks **(D)**. **(E)** TEM image of MSNs cocultured with rBMMSCs in MSCM at 1 week. MSCM, mesenchymal stem cell medium; PBS, phosphate-buffered saline; rBMMSCs, rat bone marrow mesenchymal stem cells.

Protein loading and release of MSN-DMEP

MSNs were mixed with excess DMEP at 4°C for 24 h. The maximum loading of total protein of MSNs was 610 ± 11 μg/mg in nDMEP and 673 ± 53 μg/mg in bDMEP (Fig. 5A). The amount of TGF-β1 loaded in MSNs was 5.23 ± 1.31 ng/mg in nDMEP and 16.81 ± 3.87 ng/mg in bDMEP (Fig. 5B). The maximum loading of Cyto-C in MSNs was 442.5 ± 19.0 μg/mg. After being immersed in PBS at 1 mg/mL, 45.64% ± 3.49% of Cyto-C was gradually released from MSNs in 28 days (Fig. 5C).

Cell viability of rBMMSCs cultured with MSN-DMEP

After 7 days of culture, 1 mg/mL of MSNs decreased the cell number of rBMMSCs. MSN-nDMEP decreased the cell number at days 1, 3, and 5, but had no inhibition at day 7. However, MSN-bDMEP decreased the cell number at days 1, 3, and 5, but increased the cell number at day 7 (Fig. 6).

MSN-DMEP promoted chondrogenic differentiation of rBMMSCs

The expression of chondrogenic differentiation-related genes (*Acan*, *Col2*, *Col10*, and *Sox9*) was detected by real-time PCR after rBMMSCs were cocultured with MSN, MSN-nDMEP, and MSN-bDMEP for 14 days. CIM was used as a negative control, and CIM with 10 ng/mL TGF-β1 was used as a positive control. The MSN-bDMEP group had the highest expression of *Acan* compared with the other groups. The expression of *Acan* in the MSN-nDMEP group was significantly higher than that in the control, TGF-β, and MSN groups. There was no significant difference between the control and MSN groups in *Acan* expression (Fig. 7A). No statistically significant difference was detected in *Col2* expression among the control, MSN, and MSN-nDMEP groups.

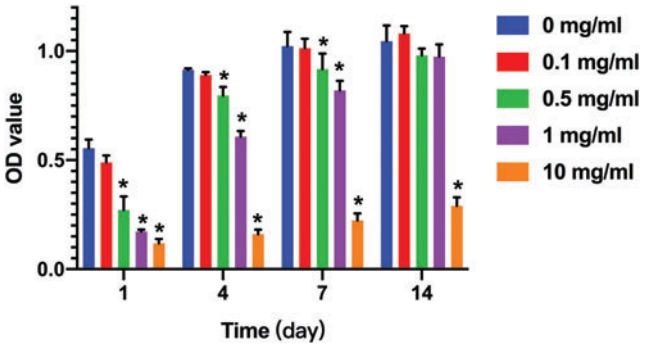

FIG. 4. Cell viability of rBMMSCs cultured with MSNs detected by CCK-8 assay. Each bar represents the mean ± SD. *Indicates a significant difference compared with the control group (0 mg/mL; $p < 0.05$). CCK-8, cell counting kit-8. Color images are available online.

The MSN-bDMEP group had a significantly higher *Col2* expression than the abovementioned groups, but a significantly lower *Col2* expression than the positive control (TGF-β) group (Fig. 7B). *Col10* expression did not differ statistically among the control, TGF-β, MSN, and MSN-nDMEP groups. The expression of *Col10* in MSN-bDMEP was significantly higher than that in the other groups (Fig. 7C). The greatest amount of *Sox9* expression was observed in the MSN-bDMEP group, with less *Sox9* expression in the TGF-β and MSN-nDMEP groups than in the MSN group, and the lowest expression was observed in the control group (Fig. 7D).

MSN-DMEP promoted cartilaginous matrix formation of rBMMSCs

The chondrogenic pellets formed by rBMMSCs were fixed and histologically stained to observe the formation of cartilage-specific matrix components (Fig. 8). Alcian blue and safranin O staining showed that the pellets in the control and MSN groups were looser than those in the TGF-β, MSN-nDMEP, and MSN-bDMEP groups, and no red-staining or dark blue-staining matrix was detected. The positive control (TGF-β) group showed abundant cartilage-specific matrix with strong red and dark blue staining and a cartilage-lacuna-like structure, which was characteristic of a cartilage matrix. MSN-bDMEP stimulation induced chondrogenic differentiation of rBMMSCs similar to that induced by TGF-β with strong red and alcian blue staining and cartilage-specific matrix formation.

The MSN-nDMEP group showed less and uneven cartilage matrix deposition than the TGF-β and MSN-bDMEP groups. The staining in the central region of the pellet was strong, while light staining was observed in the surface layer, indicating localized cartilage formation. The results of histological staining indicated that rBMMSCs in pellets

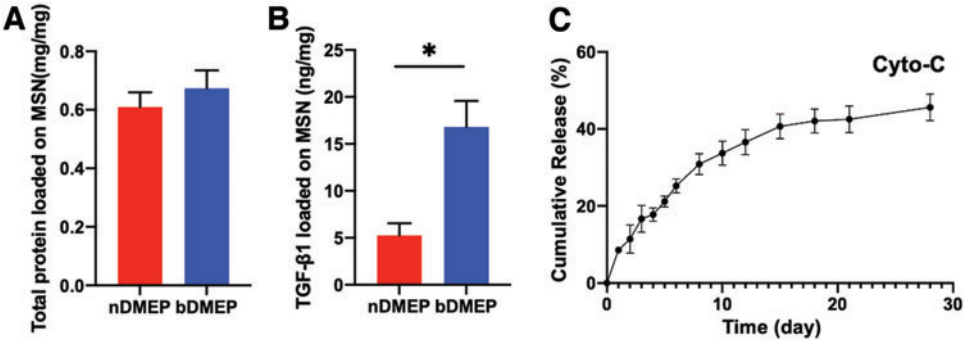

FIG. 5. Protein loading and release performance of MSNs. **(A)** Amount of total protein in nDMEP and bDMEP loaded on MSNs. **(B)** Amount of TGF-β1 in nDMEP and bDMEP loaded on MSNs. **(C)** Protein release curve of MSNs. Each bar represents the mean ± SD. $^*p < 0.05$. Color images are available online.

could differentiate toward the chondrogenic direction and synthesize a cartilaginous matrix under MSN-DMEP induction, especially bDMEP.

MSN-bDMEP promoted cartilage regeneration in articular cartilage defects

Histology staining results at 12 weeks postsurgery are presented in Figure 9. The HE staining results showed that in the blank and collagen (C) groups, fibrous tissues were seen in the defect area, and the thickness was thinner than the adjacent normal cartilage (Fig. 9A1–4). Alcian blue staining and safranin O-fast green staining of newly generated tissue were slight, indicating that the blank group and C group had a lower proteoglycan and glycosaminoglycan content. In addition, the collagen fibrils were randomly arranged (Fig. 9B1–4, C1–4). The collagen+MSN (C+S) group formed a deeply alcian blue-stained cartilage-like tissue with cartilage lacuna (Fig. 9A5, A6, B5, B6).

Safranin O-fast green staining showed that the neogenerated cartilage-like tissue was unclearly stratified and the chondrocytes and collagen fibrils were arranged randomly. The red staining is slighter than the adjacent normal cartilage (Fig. 9C5, C6). In the collagen+MSN+bDMEP (C+S+D) group, the newly formed cartilage-like tissue was thicker than the other three groups (Fig. 9A7, A8). Alcian blue staining showed abundant dark blue cartilage matrix with cartilage lacunae bonding to the adjacent cartilage (Fig. 9B7, B8). Safranin O-fast green staining showed that the new cartilage had obvious three zones and the tidemark. In the superficial zone (SZ), the chondrocytes were flat and the collagen orientation was parallel to the surface. The slightest red staining in this zone means that this area had the lowest concentration of proteoglycans.

The middle zone (MZ) showed round chondrocytes and randomly arranged collagen fibrils. The intense red staining indicated abundant proteoglycans. In the deep zone (DZ), chondrocytes and collagen fibrils are arranged in columns perpendicular to the joint surface. Tidemark was seen below the DZ. These results indicated that MSN-bDMEP promoted cartilage regeneration *in vivo*.

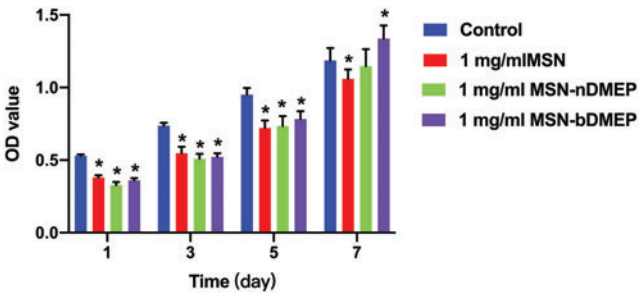

FIG. 6. Cell viability of rBMMSCs cultured with MSN-DMEP detected by CCK-8 assay. Each bar represents the mean ± SD. *Indicates a significant difference compared with the control group ($p < 0.05$). Color images are available online.

Discussion

DMEP contains a variety of growth factors related to cartilage regeneration, such as TGF-β,[8,9,11] IGF-1,[9,11] IGF-2,[10] BMP,[13,14] bFGF,[12] and PDGF.[30,31] Our results showed that the concentrations of TGF-β1, bFGF, and IGF-1 in DMEP were, respectively, high above 1 ng/mL, while the concentrations of TGF-β3, BMP-2, BMP-9, and VEGF were below 100 pg/mL. The dosage of growth factors is related to their chondrogenesis-promoting effect. It was found that in an *in vitro* model, 10 ng/mL of TGF-β1 could induce the cartilage matrix extracellularly formed abundantly and homogeneously, whereas only few of the cartilage extracellular matrix formed after chondrogenic induction with 1 and 0.5 ng/mL of TGF-β1.[32] Moreover, 1 ng/mL of IGF-1 had no obvious effect of proliferation in BMMSCs, but IGF-1 at the concentration of 10 ng/mL and above facilitated BMMSC proliferation and reached the optimum condition at 50 ng/mL.[33]

Solchaga *et al.* found that 1–10 ng/mL of bFGF promoted both MSC proliferation and chondrogenic differentiation.[34] In addition, Majumdar *et al.* found that BMP-2 and BMP-9 at the concentration of 100 ng/mL promoted chondrogenic differentiation of human multipotential mesenchymal cells.[35] The minimum effective concentration of growth factors was approximately above 1 ng/mL, which suggests that TGF-β1, IGF-1, and bFGF in DMEP might play a major role in cartilage regeneration. Furthermore, different growth factors have synergistic effects on chondrogenesis. Studies have shown a significant increase in cartilage matrix formation when IGF-1 is combined with the TGF-β superfamily such as TGF-β1, BMP-2, and BMP-7.[33,36] The combination of TGF-β1 and bFGF was demonstrated to synergistically promote the chondrogenic differentiation of periotic mesenchyme *in vitro*.[15] DMEP, as a complex of several growth factors, may show a superior effect than a single growth factor, providing new hope for promoting articular cartilage regeneration.

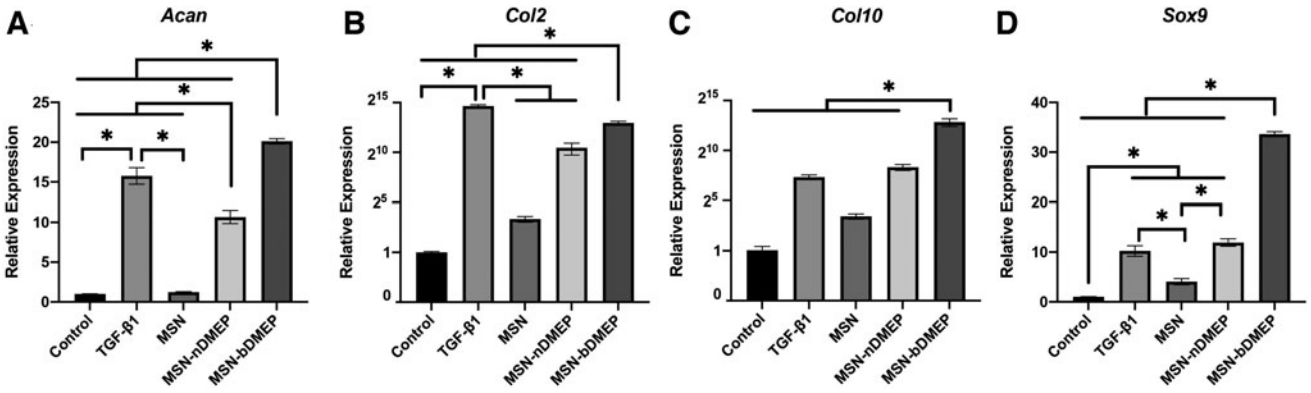

FIG. 7. Chondrogenic differentiation of rBMMSCs cultured with MSN-DMEP for 2 weeks. **(A)** Acan gene expression **(B)** Col2 gene expression **(C)** Col 10 gene expression **(D)** Sox9 gene expression. *Indicates a significant difference between groups ($p < 0.05$).

DMEP is usually extracted under neutral conditions.[37] In this study, DMEP extracted in basic solution significantly increased the concentration of active TGF-β1, IGF-1, and bFGF compared with that in nDMEP. TGF-β1 is synthesized as latent complexes. The mature TGF-β1 is noncovalently associated with a disulfide-bonded complex of the N-terminal remnant of the TGF-β1 latency-associated peptide (LAP). Human dentin contains both mature TGF-β1 and latent TGF-β1, which bind to LAP.[38,39] Changes in pH can activate the TGF-β homodimer by dissociating LAP, thereby exerting its biological effects.[40] Our previous studies had tested the effects of alkaline treatment at different pH on the activation of endogenous latent TGF-β1 and its biological function, and found that alkaline conditioning at pH 10 was able to activate endogenous latent TGF-β1, while the active TGF-β1 may lose its biological activity at pH 11 or above.[41] The pH 10-activated endogenous TGF-β1 exhibited good bioactivity by promoting BMMSC recruitment and early differentiation.[41]

Other studies also reported that an alkaline environment helps the release of growth factors from the dentin matrix, such as IGF-1.[42,43] IGF-1 could be stable when released in an alkaline environment (pH 10.1).[44] BMP-2, a member of the TGF-β family, was also reported to be able to retains its biological activity at pH 7–11.[45] In addition, the protein conformation of bFGF was able to keep stable at pH as high as 9.0.[46] Given the importance of TGF-β, IGF-1, and bFGF to cartilage regeneration,[16] alkaline conditioning might improve the chondroinductive ability of DMEP. However, the exact mechanism underlying the effect of alkalinity on the biological effects of these proteins requires further investigation.

This study revealed that MSNs were highly efficient nanocarriers for the loading and delivery of proteins. At 37°C, MSNs could sustainably release ~40–50% of the total loaded protein at 28 days. The physicochemical characteristics of MSNs determine their adsorption capacity for DMEP. In this study, there were significant differences in the loading amount of TGF-β1 in bDMEP and nDMEP by MSN. The ratio of loaded TGF-β1 to loaded total protein in MSNs was higher than that in the original DMEP extract, indicating that our designed MSNs with proper physicochemical properties can selectively load more TGF-β1 in DMEP. MSN loaded with chondrogenic-related growth factors in DMEP may be due to the matched pore size and electrostatic attraction.

Previous research has found that the ideal pore size of the material should be three to five times the diameter of the loaded protein.[18] Chondrogenic-related growth factors in DMEP, such as active TGF-β1, bFGF, and IGF-1, have a molecular weight between 5 and 20 kDa and a diameter of ~2–4 nm.[47–49] The MSNs designed in this study had a pore size of 6 nm, which is favorable for the loading of the above growth factors. Moreover, the MSNs had a radial pore

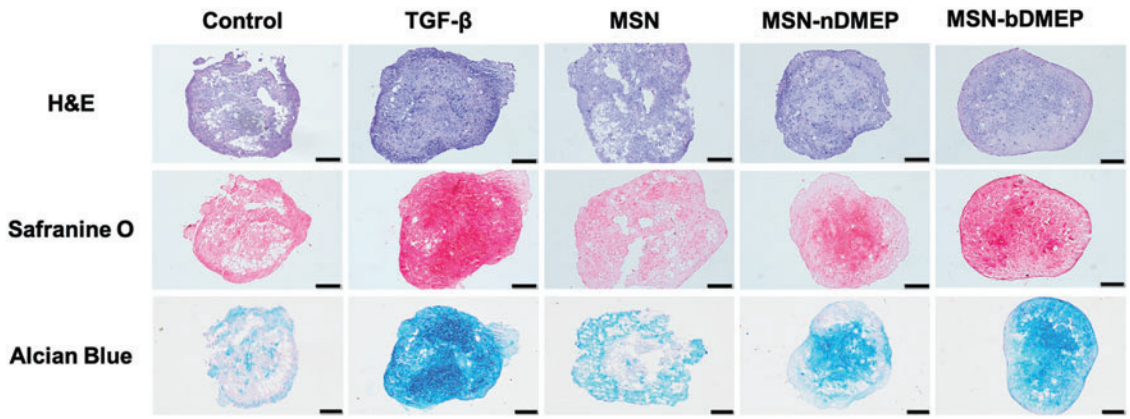

FIG. 8. Histological staining of chondrogenic pellets was conducted after 21 days of chondrogenic differentiation. Scale bar = 200 μm. Color images are available online.

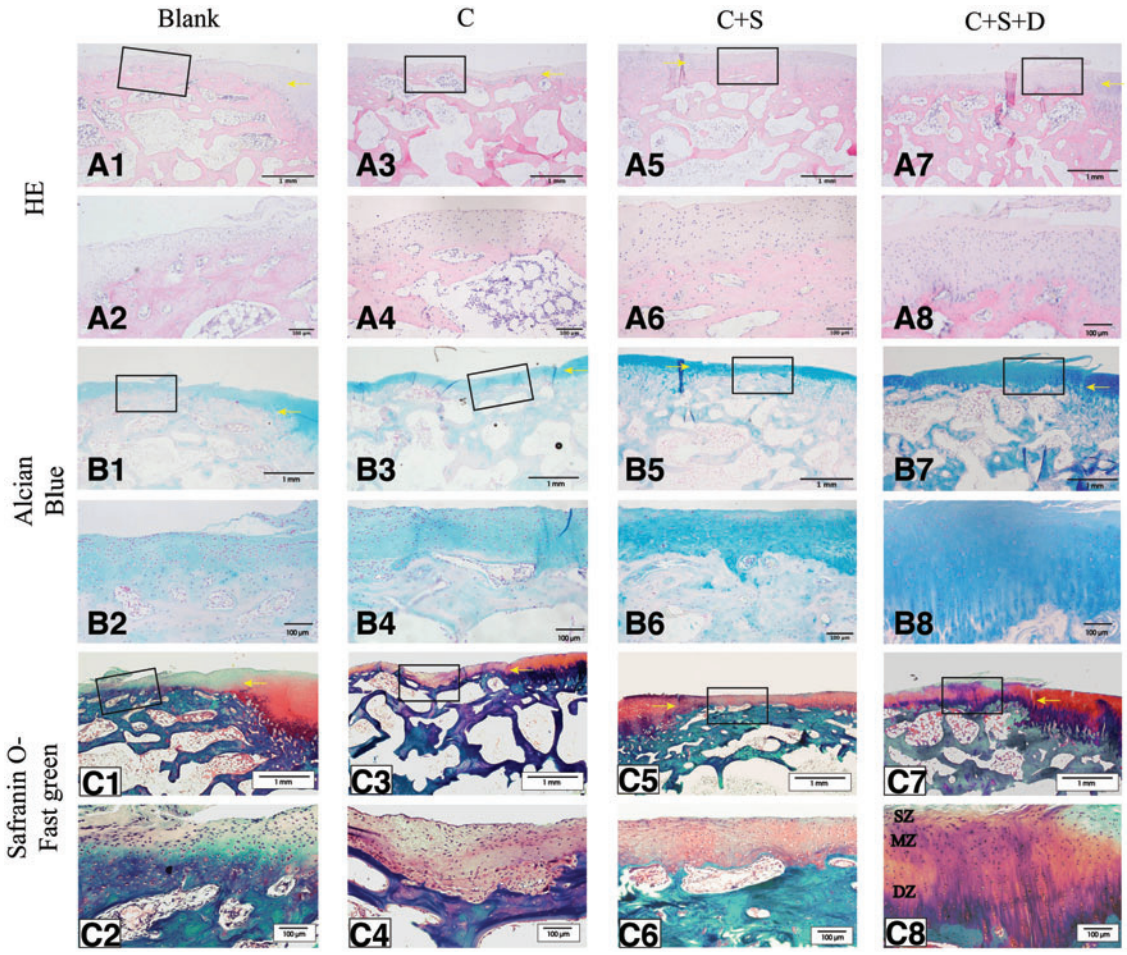

FIG. 9. *In vivo* effects of MSN-bDMEP on cartilage regeneration in a rabbit osteochondral defect model at 12 weeks. **(A1–A8)** HE staining. **(B1–B8)** Alcian blue staining. **(C1–C8)** Safranin O-fast green staining. Areas indicated in *boxes* are magnified below the respective images. *Yellow arrows* indicate the junction of defect area and normal cartilage. DZ, deep zone; HE, hematoxylin and eosin; MZ, middle zone; SZ, superficial zone. Color images are available online.

structure with a high surface area and negative charges. These characteristics further enhanced the physical adsorption of growth factors by MSNs.[19,20] The release of DMEP in MSNs is strongly associated with the degradation of MSNs.[50] MSNs with mesoporous structures have a higher surface area in contact with water than solid silica particles, resulting in faster degradation and improved drug release.[22]

We also found that the degradation rate of MSNs cocultured with rBMMSCs was faster than that in PBS, which may facilitate the release of loaded proteins and exert their biological effects. It may be possible to regulate protein release from silica-based materials through controlled erosion.[51] A model protein with a similar size to growth factors has been successfully used to simulate the loading and release of the growth factors from MSNs.[52] Santos at el. found that porous silica loaded with different concentrations of model protein shared similar release curves and the release amount was dose dependent.[53] Since MSNs in the bDMEP group loaded more TGF-β1 than those in the nDMEP group, MSN-bDMEP should release more TGF-β1 than MSN-nDMEP, but with similar release curves with the model protein Cyto-C.

It was reported that MSNs possessed low toxicity *in vitro* against the various cell lines.[54] The major toxicity associated with silica is due to its surface chemistry (silanol groups), which can interact with the membrane components leading to the lysis of cells and the consequent leaking of the cellular components.[55] Mesoporous silica exhibits a lower toxicity compared with nonporous silica that could be attributed to the lower density of silanol groups on the surface of these structures.[56] In our cell viability experiment, MSNs at concentration of 0.1, 0.5, and 1 mg/mL exhibited decreasing cytotoxic activity at day 14. The reason may be that MSNs degraded gradually and the volume of the pore spaces increased, which may lead to the reduced surface silanol density and overall cell-accessible surface.

The present study showed that MSN-bDMEP significantly promoted the proliferation of rBMMSCs, the expression of chondrogenesis-related genes, and the formation of cartilage-like matrix. These results suggested that MSN-DMEP could slowly release chondrogenesis-related growth factors that were maintained at effective concentrations for a long time. MSN-bDMEP had a better chondrogenic effect than nDMEP. This may be associated with the increased concentrations of TGF-β1, bFGF, and IGF-1 in MSN-bDMEP.

In this study, the use of MSN-bDMEP effectively lowered the dose and frequency requirement of TGF-β1. We

supplied 10 ng/mL of TGF-β1 every other day in the positive control (TGF-β1) group, and the total amount of TGF-β1 added was 20 ng per pellet throughout the culture period. While in the MSN-nDMEP and MSN-bDMEP groups, the total TGF-β1 loaded in MSNs was ~1 and 3 ng per pellet, respectively, and no repeated administration was needed. MSN-bDMEP achieved a chondrogenic effect similar to that of the TGF-β1 group, suggesting that the complex growth factors in DMEP may have synergistic chondrogenic effects superior to those of TGF-β1 alone. Using a sustained-release system to deliver growth factors can achieve chondrogenic effects similar to the traditional cell pellet culture methods, but does not require repeated administration and requires a much lower dose.[57]

Furthermore, in the initial stage of chondrogenesis, mesenchymal stem cells condense and then differentiate into chondrocytes.[58] However, chondrogenic cell pellets with high cell density are subject to diffusive gradients of metabolites, gases, and growth factors, resulting in growth inhibition and spatial differentiation heterogeneity inside the pellet.[59–61] Mixing MSNs into the rBMMSC pellet reduced its compactness. It is conducive to cell proliferation and the formation of extracellular matrix. In addition, MSNs within chondrogenic pellets released chondroinductive stimuli from inside, which may favor the integral and synchronized differentiation of cells.

Due to the low stability and rapid diffusion of growth factors *in vivo*, maintaining effective local concentrations of growth factors is important for their biological effects. In the *in vivo* study, we used MSNs with fully loaded bDMEP (MSN-bDMEP) and the maximum concentration of MSNs that did not affect collagen gelation. Accordingly, the amount of TGF-β in 60 μL of collagen I with 10 mg/mL of MSN-bDMEP is ~10 ng and the concentration of TGF-β in C+S+D was about 160 ng/mL, which was the effective concentration to induce cartilage regeneration *in vivo*. In previous studies, TGF-β1 at a concentration of 20–2000 ng/mL was utilized *in vivo* and obtained favorable cartilage repair effects.[62–65]

The result showed that MSN-bDMEP could induce the formation of cartilage-like structure in rabbit knee-joint articular cartilage defect, indicating that MSN-bDMEP was able to promote cartilage regeneration *in situ*. The results of the *in vivo* study could be corroborated with the results of *in vitro* cytology experiments.

In this study, we found that the hypertrophy marker *Col10* was highly expressed in the MSN-bDMEP group. Further research on the optimal concentration of DMEP is needed in subsequent studies. Simultaneously, modifying MSNs to obtain relatively stable degradation and release rates is particularly important to enhance the production of the extracellular matrix of cartilage and inhibit hypertrophy.

Conclusion

DMEP is a mixture of a variety of proteins. In this study, we improved the extraction of DMEP by basic conditioning, which increased the content and activity of chondrogenic-related growth factors compared with the traditional neutral solution extraction method. Then, our designed MSN with suitable physicochemical characteristics can load and control the release of chondrogenic-related growth factors in DMEP, thereby promoting the chondrogenesis of rBMMSCs. MSNs loaded with DMEP have the potential to be applied to cartilage regeneration as an alternative to expensive synthetic growth factors.

Acknowledgments

The authors thank the National Natural Science Foundation of China (81700953, 81870753, and 81901054), Open Funding of Guangdong Provincial Key Laboratory of Stomatology (KF2021120104), and the China Postdoctoral Science Foundation (2019M660010) for funding this research.

Authors' Contributions

S.M.: Conceptualization, methodology, investigation, visualization, writing—original draft, and writing—review and editing. S.W.: Conceptualization, methodology, funding acquisition, and writing—review and editing. Y.N.: Methodology and resources. J.W.: Investigation. P.J.: Investigation. J.Z.: Funding acquisition. Y.D.: Project administration, supervision, funding acquisition, and writing—review and editing.

Disclosure Statement

No competing financial interests exist.

Funding Information

This work was supported by the National Natural Science Foundation of China (81700953, 81870753, and 81901054), Open Funding of Guangdong Provincial Key Laboratory of Stomatology (KF2021120104), and the China Postdoctoral Science Foundation (2019M660010).

Supplementary Material

Supplementary Data
Supplementary Table S1

References

1. Correa, D., and Lietman, S.A. Articular cartilage repair: current needs, methods and research directions. Semin Cell Dev Biol **62,** 67, 2017.
2. Ge, Z., Li, C., Heng, B.C., Cao, G., and Yang, Z. Functional biomaterials for cartilage regeneration. J Biomed Mater Res A **100,** 2526, 2012.
3. Fortier, L.A., Barker, J.U., Strauss, E.J., McCarrel, T.M., and Cole, B.J. The role of growth factors in cartilage repair. Clin Orthop Relat Res **469,** 2706, 2011.
4. Shi, S., Mercer, S., Eckert, G.J., and Trippel, S.B. Growth factor regulation of growth factors in articular chondrocytes. J Biol Chem **284,** 6697, 2009.
5. Muramatsu, T., Hamano, H., Fukumashi, K., *et al.* An experimental study of chondrogenesis and osteogenesis in rat submandibular gland induced by implantation of demineralized dentin. Bull Tokyo Dent Coll **34,** 15, 1993.
6. Yagihashi, K., Miyazawa, K., Togari, K., and Goto, S. Demineralized dentin matrix acts as a scaffold for repair of articular cartilage defects. Calcif Tissue Int **84,** 210, 2009.

7. Somerman, M., Nathanson, M., Sauk, J., and Manson, B. Human dentin matrix induces cartilage formation in vitro by mesenchymal cells derived from embryonic muscle. J Dent Res **66,** 1551, 1987.
8. Chun, S.Y., Lee, H.J., Choi, Y.A., *et al.* Analysis of the soluble human tooth proteome and its ability to induce dentin/tooth regeneration. Tissue Eng Part A **17,** 181, 2011.
9. Park, E.-S., Cho, H.-S., Kwon, T.-G., *et al.* Proteomics analysis of human dentin reveals distinct protein expression profiles. J Proteome Res **8,** 1338, 2009.
10. Finkelman, R.D., Mohan, S., Jennings, J.C., Taylor, A.K., and Baylink, D.J. Quantitation of growth factors IGF-I, SGF/IGF-II, and TGF-β in human dentin. J Bone Miner Res **5,** 717, 2009.
11. Jágr, M., Eckhardt, A., Pataridis, S., and Mikšík, I. Comprehensive proteomic analysis of human dentin. Eur J Oral Sci **120,** 259, 2012.
12. Roberts-Clark, D.J., and Smith, A.J. Angiogenic growth factors in human dentine matrix. Arch Oral Biol **45,** 1013, 2000.
13. Bessho, K., Tanaka, N., Matsumoto, J., Tagawa, T., and Murata, M. Human dentin-matrix-derived bone morphogenetic protein. J Dent Res **70,** 171, 1990.
14. Bessho, K., Tagawa, T., and Murata, M. Purification of rabbit bone morphogenetic protein derived from bone, dentin, and wound tissue after tooth extraction. J Oral Maxillofac Surg **48,** 162, 1990.
15. Frenz, D.A., Liu, W., Williams, J.D., *et al.* Induction of chondrogenesis: requirement for synergistic interaction of basic fibroblast growth factor and transforming growth factor-beta. Development **120,** 415, 1994.
16. Toh, W.S., Liu, H., Heng, B.C., *et al.* Combined effects of TGFβ1 and BMP2 in serum-free chondrogenic differentiation of mesenchymal stem cells induced hyaline-like cartilage formation. Growth Factors **23,** 313, 2005.
17. Yaeger, P.C., Masi, T.L., de Ortiz, J.L.B., *et al.* Synergistic action of transforming growth factor-β and insulin-like growth factor-I induces expression of type II collagen and aggrecan genes in adult human articular chondrocytes. Exp Cell Res **237,** 318, 1997.
18. Gao, S., Wang, Y., Diao, X., Luo, G., and Dai, Y. Effect of pore diameter and cross-linking method on the immobilization efficiency of *Candida rugosa* lipase in SBA-15. Bioresour Technol **101,** 3830, 2010.
19. Young, S., Wong, M., Tabata, Y., and Mikos, A.G. Gelatin as a delivery vehicle for the controlled release of bioactive molecules. J Control Release **109,** 256, 2005.
20. Rabinow, B.E. Nanosuspensions in drug delivery. Nat Rev Drug Discov **3,** 785, 2004.
21. Li, Z., Barnes, J.C., Bosoy, A., Stoddart, J.F., and Zink, J.I. Mesoporous silica nanoparticles in biomedical applications. Chem Soc Rev **41,** 2590, 2012.
22. Yamada, H., Urata, C., Aoyama, Y., *et al.* Preparation of colloidal mesoporous silica nanoparticles with different diameters and their unique degradation behavior in static aqueous systems. Chem Mater **24,** 1462, 2012.
23. Miao, G., Li, Z., Meng, Y., *et al.* Preparation, characterization, in vitro bioactivity and protein loading/release property of mesoporous bioactive glass microspheres with different compositions. Adv Powder Technol **30,** 1848, 2019.
24. Wu, Q., Liu, C., Fan, L., *et al.* Heparinized magnetic mesoporous silica nanoparticles as multifunctional growth factor delivery carriers. Nanotechnology **23,** 485703, 2012.
25. Croissant, J.G., Fatieiev, Y., and Khashab, N.M. Degradability and clearance of silicon, organosilica, silsesquioxane, silica mixed oxide, and mesoporous silica nanoparticles. Adv Mater **29,** 2017 [Epub ahead of print]; 10.1002/adma.201604634.
26. Lin, C.-Y., Yang, C.-M., and Lindén, M. Dissolution and morphology evolution of mesoporous silica nanoparticles under biologically relevant conditions. J Colloid Interface Sci **608,** 995, 2022.
27. Lin, B., Hu, H., Deng, Z., *et al.* Novel bioactive glass cross-linked PVA hydrogel with enhanced chondrogenesis properties and application in mice chondrocytes for cartilage repair. J Non-Cryst Solids **529,** 119594, 2020.
28. Ren, L., Cong, N., Han, H., *et al.* The effect of sodium metasilicate on the three-dimensional chondrogenesis of mesenchymal stem cells. Dent Mater J **40,** 853, 2021.
29. Shen, D., Yang, J., Li, X., *et al.* Biphase stratification approach to three-dimensional dendritic biodegradable mesoporous silica nanospheres. Nano Lett **14,** 923, 2014.
30. Hulth, A., Johnell, O., Miyazono, K., *et al.* Effect of transforming growth factor-β and platelet-derived growth factor-BB on articular cartilage in rats. J Orthop Res **14,** 547, 1996.
31. Schmidt, M., Chen, E., and Lynch, S. A review of the effects of insulin-like growth factor and platelet derived growth factor on in vivo cartilage healing and repair. Osteoarthr Cartilage **14,** 403, 2006.
32. Johnstone, B., Hering, T.M., Caplan, A.I., Goldberg, V.M., and Yoo, J.U. In vitro chondrogenesis of bone marrow-derived mesenchymal progenitor cells. Exp Cell Res **238,** 265, 1998.
33. Longobardi, L., O'Rear, L., Aakula, S., *et al.* Effect of IGF-I in the chondrogenesis of bone marrow mesenchymal stem cells in the presence or absence of TGF-β signaling. J Bone Miner Res **21,** 626, 2006.
34. Solchaga, L.A., Penick, K., Porter, J.D., *et al.* FGF-2 enhances the mitotic and chondrogenic potentials of human adult bone marrow-derived mesenchymal stem cells. J Cell Physiol **203,** 398, 2005.
35. Majumdar, M.K., Wang, E., and Morris, E.A. BMP-2 and BMP-9 promotes chondrogenic differentiation of human multipotential mesenchymal cells and overcomes the inhibitory effect of IL-1. J Cell Physiol **189,** 275, 2001.
36. An, C., Cheng, Y., Yuan, Q., and Li, J. IGF-1 and BMP-2 induces differentiation of adipose-derived mesenchymal stem cells into chondrocytes-like cells. Ann Biomed Eng **38,** 1647, 2010.
37. Tabatabaei, F.S., Tatari, S., Samadi, R., and Moharamzadeh, K. Different methods of dentin processing for application in bone tissue engineering: a systematic review. J Biomed Mater Res A **104,** 2616, 2016.
38. Smith, A.J., Matthews, J.B., and Hall, R.C. Transforming growth factor-beta1 (TGF-beta1) in dentine matrix. Ligand activation and receptor expression. Eur J Oral Sci **106(Suppl 1),** 179, 1998.
39. Sloan, A.J., Moseley, R., Dobie, K., Waddington, R.J., and Smith, A.J. TGF-β latency-associated peptides (LAPs) in human dentin matrix and pulp. Connect Tissue Res **43,** 381, 2002.
40. Shi, M., Zhu, J., Wang, R., *et al.* Latent TGF-β structure and activation. Nature **474,** 343, 2011.
41. Wang, S., Niu, Y., Jia, P., *et al.* Alkaline activation of endogenous latent TGFβ1 by an injectable hydrogel directs cell homing for in situ complex tissue regeneration. Bioact Mater **15,** 316, 2021.

42. Graham, L., Cooper, P.R., Cassidy, N., *et al.* The effect of calcium hydroxide on solubilisation of bio-active dentine matrix components. Biomaterials **27,** 2865, 2006.
43. Tomson, P., Lumley, P., Smith, A., and Cooper, P. Growth factor release from dentine matrix by pulp-capping agents promotes pulp tissue repair-associated events. Int Endod J **50,** 281, 2017.
44. Mantripragada, V.P., and Jayasuriya, A.C. IGF-1 release kinetics from chitosan microparticles fabricated using environmentally benign conditions. Mater Sci Eng C **42,** 506, 2014.
45. Quaas, B., Burmeister, L., Li, Z., *et al.* Stability and biological activity of *E. coli* derived soluble and precipitated bone morphogenetic protein-2. Pharm Res **36,** 1, 2019.
46. Vemuri, S., Beylin, I., Sluzky, V., *et al.* The stability of bFGF against thermal denaturation. J Pharm Pharmacol **46,** 481, 1994.
47. Siwanowicz, I., Popowicz, G.M., Wisniewska, M., *et al.*, Structural basis for the regulation of insulin-like growth factors by IGF binding proteins. Structure **13,** 155, 2005.
48. Hinck, A.P., Archer, S.J., Qian, S.W., *et al.* Transforming growth factor β1: three-dimensional structure in solution and comparison with the X-ray structure of transforming growth factor β2. Biochemistry **35,** 8517, 1996.
49. Zhu, X., Komiya, H., Chirino, A., *et al.* Three-dimensional structures of acidic and basic fibroblast growth factors. Science **251,** 90, 1991.
50. He, Q., Shi, J., Zhu, M., Chen, Y., and Chen, F. The three-stage in vitro degradation behavior of mesoporous silica in simulated body fluid. Microporous Mesoporous Mater **131,** 314, 2010.
51. Yang, S.-A., Choi, S., Jeon, S.M., and Yu, J. Silica nanoparticle stability in biological media revisited. Sci Rep **8,** 1, 2018.
52. Bhattacharyya, S., Wang, H., and Ducheyne, P. Polymer-coated mesoporous silica nanoparticles for the controlled release of macromolecules. Acta Biomater **8,** 3429, 2012.
53. Santos, E.M., Radin, S., and Ducheyne, P. Sol–gel derived carrier for the controlled release of proteins. Biomaterials **20,** 1695, 1999.
54. Napierska, D., Thomassen, L.C., Lison, D., Martens, J.A., and Hoet, P.H. The nanosilica hazard: another variable entity. Part Fibre Toxicol **7,** 1, 2010.
55. Jafari, S., Derakhshankhah, H., Alaei, L., *et al.* Mesoporous silica nanoparticles for therapeutic/diagnostic applications. Biomed Pharmacother **109,** 1100, 2019.
56. Tao, Z., Toms, B.B., Goodisman, J., and Asefa, T. Mesoporosity and functional group dependent endocytosis and cytotoxicity of silica nanomaterials. Chem Res Toxicol **22,** 1869, 2009.
57. Solorio, L.D., Fu, A.S., Hernández-Irizarry, R., and Alsberg, E. Chondrogenic differentiation of human mesenchymal stem cell aggregates via controlled release of TGF-β1 from incorporated polymer microspheres. J Biomed Mater Res A **92,** 1139, 2010.
58. DeLise, A.M., Fischer, L., and Tuan, R. Cellular interactions and signaling in cartilage development. Osteoarthr Cartilage **8,** 309, 2000.
59. Mercier, N.R., Costantino, H.R., Tracy, M.A., and Bonassar, L.J. Poly (lactide-co-glycolide) microspheres as a moldable scaffold for cartilage tissue engineering. Biomaterials **26,** 1945, 2005.
60. Malda, J., Van Blitterswijk, C., Van Geffen, M., *et al.* Low oxygen tension stimulates the redifferentiation of dedifferentiated adult human nasal chondrocytes. Osteoarthr Cartilage **12,** 306, 2004.
61. Futrega, K., Robey, P.G., Klein, T.J., Crawford, R.W., and Doran, M.R. A single day of TGF-β1 exposure activates chondrogenic and hypertrophic differentiation pathways in bone marrow-derived stromal cells. Commun Biol **4,** 1, 2021.
62. Mierisch, C.M., Cohen, S.B., Jordan, L.C., *et al.* Transforming growth factor-β in calcium alginate beads for the treatment of articular cartilage defects in the rabbit. Arthroscopy **18,** 892, 2002.
63. Singh, N., Shiwani, S., Singh, G., *et al.* TGF-β1 improves articular cartilage damage in rabbit knee. Pak Vet J **32,** 412, 2012.
64. Wang, W., Li, B., Yang, J., *et al.* The restoration of full-thickness cartilage defects with BMSCs and TGF-beta 1 loaded PLGA/fibrin gel constructs. Biomaterials **31,** 8964, 2010.
65. Fan, H., Hu, Y., Qin, L., *et al.* Porous gelatin–chondroitin–hyaluronate tri-copolymer scaffold containing microspheres loaded with TGF-β1 induces differentiation of mesenchymal stem cells *in vivo* for enhancing cartilage repair. J Biomed Mater Res A **77A,** 785, 2006.

Address correspondence to:
Sainan Wang, PhD
Department of Cariology and Endodontology
Peking University School and Hospital of Stomatology
22 Zhongguancun Nandajie, Haidian District
Beijing 100081
P.R. China

E-mail: bdkqwsn@bjmu.edu.cn

Yanmei Dong, DDS, PhD
Department of Cariology and Endodontology
Peking University School and Hospital of Stomatology
22 Zhongguancun Nandajie, Haidian District
Beijing 100081
P.R. China

E-mail: kqdongyanmei@bjmu.edu.cn

Received: March 1, 2022
Accepted: April 25, 2022
Online Publication Date: July 22, 2022